

Nanopackaging: Nanotechnologies & Electronics Packaging

Part D ECAs, Simulation, & Nanoelectronics Packaging

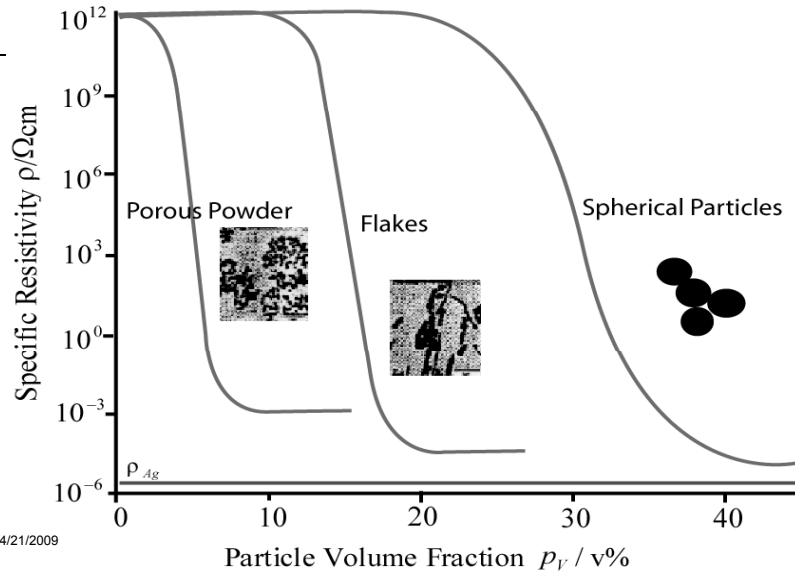
James E. Morris
Department of Electrical & Computer Engineering,
Portland State University, Portland, Oregon, USA
j.e.morris@ieee.org



Nanotechnologies in ECAs

- ECA/ICA/ACA/ACP/ACF/NCA !!!!
- ICAs
 - Nanoparticles
 - Sintering
 - Surface treatments
- ACAs, NCAs, & miscellaneous
- CNTs
- Microvias

Nanoparticles



4/21/2009

3

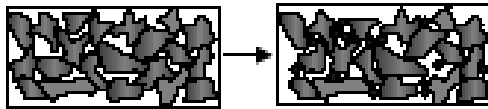


Figure 5. Schematic change of conduction path: upon introduction of nano:

Ag nanoparticles added to Ag-ICA

[Fan/Su/Qu/Wong ECTC'04]

4/21/2009

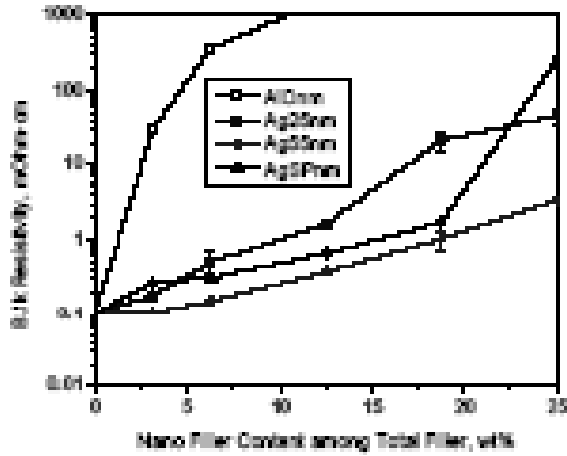


Figure 6. Resistivity vs. nano filler content for ECA with a total filler loading of 50wt% by weight

Ag nanoparticles added

Fan/Su/Qu/Wong [ECTC 2004]

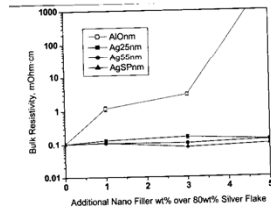
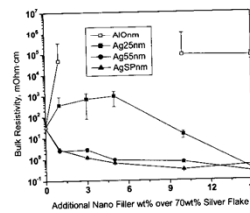


Figure 8. Resistivity vs. extra nano filler content for ECAs with a constant total silver flake loading of 80wt%



4/21/2009
Figure 9. Resistivity vs. extra nano filler content for ECAs with a constant total silver flake loading of 70wt%

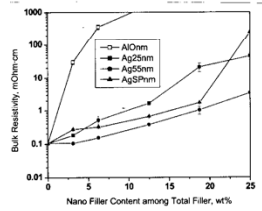


Figure 6. Resistivity vs. nano filler content for ECAs with a total filler loading of 80wt% by weight

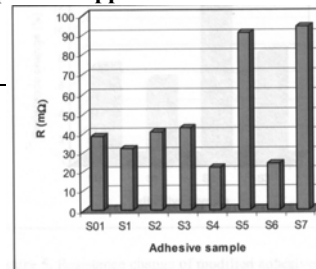
- 80% Ag + nanoparticles: no effect
- 70% Ag + nanoparticles: percolation threshold
- Ag more effective as flakes

5

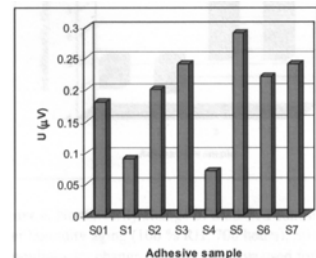
ICA: Mach, Richter, & Pietrikova Proc. ISSE 2008 Paper D003 pp. 230-235

Addition of Ag nanoparticles

Specimen	Nanoparticles Dimensions (nm)	Concentration % (wt.)	Processing
S1	(3 - 55)	10	Ag flakes substituted with Nanoparticles
S2	(3 - 55)	20	
S3	(3 - 55)	30	
S4	(80 - 100)	3.8	Nanoparticles added
S5	(6 - 8)	3.8	
S6	(80 - 100)	7.4	
S7	(6 - 8)	7.4	
S01	Bis-phenol epoxy resin; 75 wt% Ag flakes 6-8μm		



I-V Non-linearity



4/21/2009

Nanoparticle inclusion in epoxy: $AgNO_3$

[Wong et al, ECTC'06]

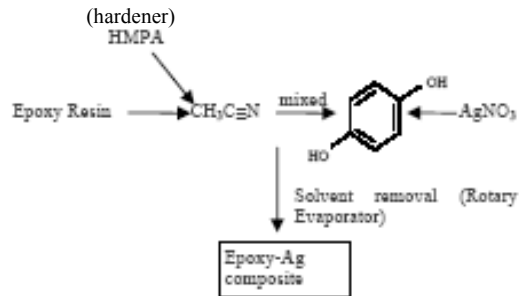


Fig. 4 Schematic illustration of the preparation of the *in-situ* conductive adhesives

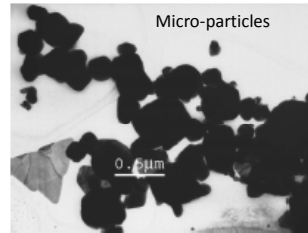


Fig. 9 Silver particles *in-situ* formed in cycloaliphatic epoxy matrix.

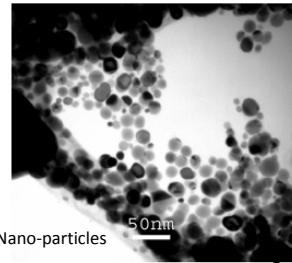


Fig. 10 Silver nanoparticles *in-situ* formed in the cycloaliphatic epoxy matrix in the presence of HMPA

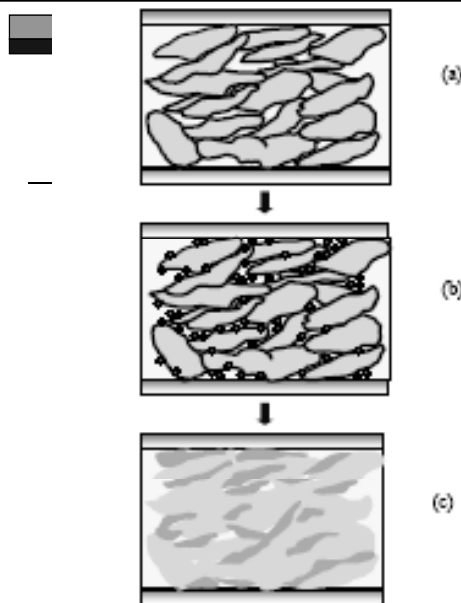


Figure 1. Schematic of particles and flakes between the metal and pads. (a) is conductive adhesives with silver flakes as fillers; (b) is conductive adhesives with both flakes and nanoparticles as fillers; (c) is conductive adhesives with sintered particles among flakes as fillers.

Nanoparticle Sintering

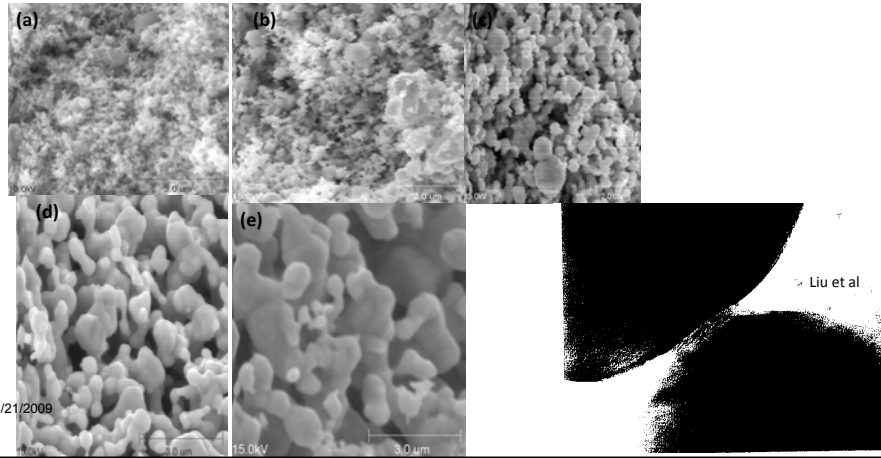
[Wong et al, ECTC'06]

Isotropic Conductive Adhesives (ICAs)

20nm-sized Ag particles annealed at different temperatures for 30 minutes:
 (a) room temperature (no annealing); (b) annealed at 100°C; (c) annealed at 150°C; (d) annealed at 200°C and (e) annealed at 250°C.

(Markers: (a) 3µm (b) 2µm (c) 2µm (d) 3µm (e) 3µm)

Lu et al



Das & Egitto

ICA Microvia Fill (PWB)

75°C micro/nano Ag sintering

4/21/2009

Endicott Interconnects Steve Harban EHT = 15.00 kV Signal A = SE2 Date 21 Aug 2006 WD = 5 mm Stage at T = 45.0 ° Mag = 6.00 K X

Nano-particle sintering

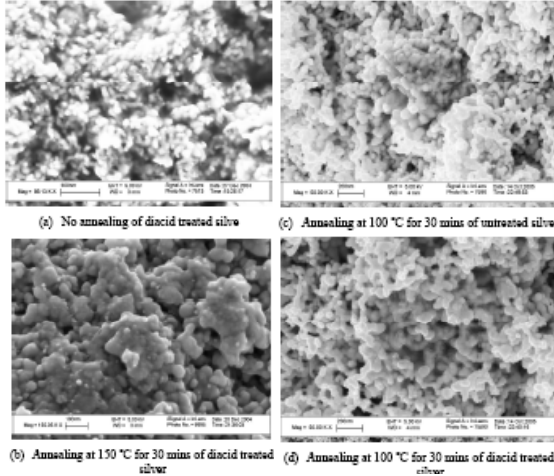


Figure 4. Comparison of the morphologies of silver nanoparticles without treatment and treated by diacids before and after annealing at 100°C and 150°C for 30 mins.

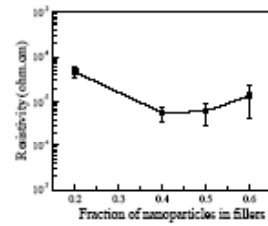
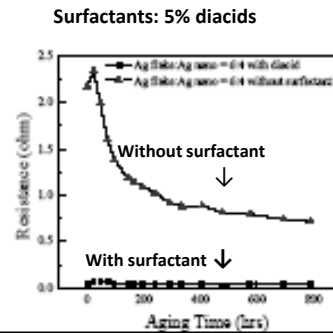


Figure 5. The bulk resistivity of the isotropic conductive adhesives with 5wt% diacids as surfactants



Stearic acid can be removed/replaced by short-chain dicarboxylic acids, with strong affinity for Ag surface (e.g. malonic acid) [Li/Moon/Li/Wong ECTC 2004]

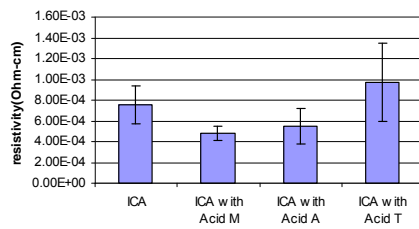


Figure 5 Effects of different dicarboxylic acids on the conductivity of ICA

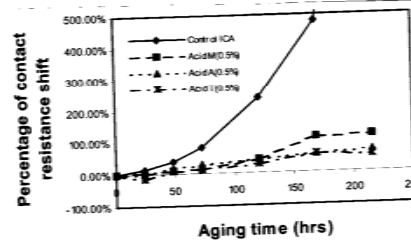
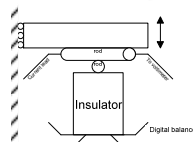
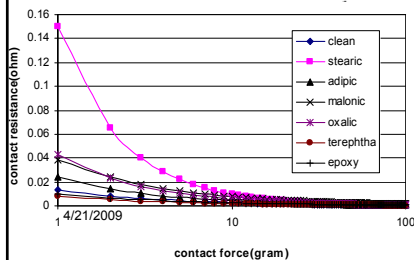


Figure 6 Contact Resistance Shifts of ECAs with and without dicarboxylic acids



Experimental resistances with short-chain acids

[Qu - APM'05]

Anisotropic Conductive Adhesive (ACA) Enhancement

(Rongwei Zhang et al ECTC'08)

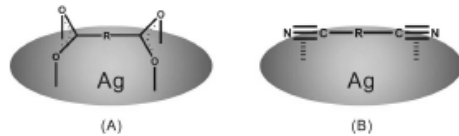
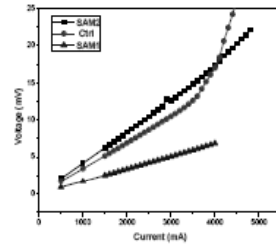


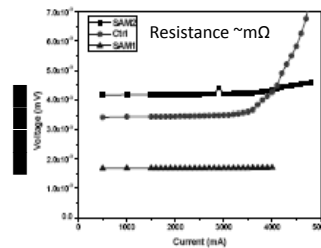
Figure 5 Alignments of SAM1 and SAM2 on a submicron-sized Ag particle surface.

SAM-1:
 "Molecular wires"
 Oxide reduction
 Lower resistance
 Higher max current

4/21/2009



(a)

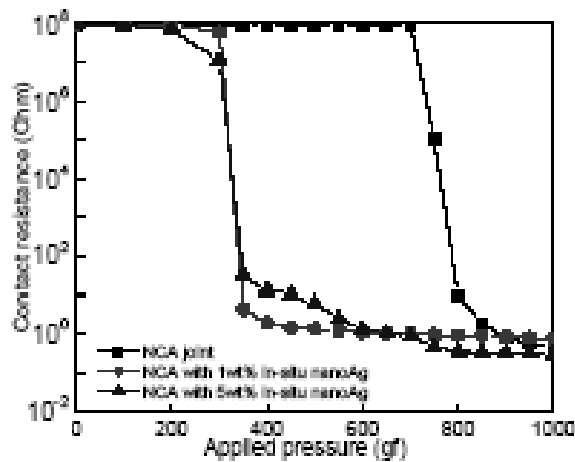


(b)

Figure 8 (a) I-V curve of ACA filled with Ag particles (ChI), SAM1-treated Ag particles and SAM2-treated Ag particles; (b) Corresponding I-R curves.

10-20 nm nano-Ag fillers for NCAs

(AgNO₃ added to polymer) [Li/Moon/Wong ECTC'06]



4/21/2009

Fig. 12 Influence of pressure on the contact resistance of NCA joints with and without *in-situ* formed nano-Ag fillers.

14

CNT-PP
 (petroleum pitch)
 composite
 (C mesophase)
 fillers for
 conductive pastes
 [Bondar et al, ECTC'05]

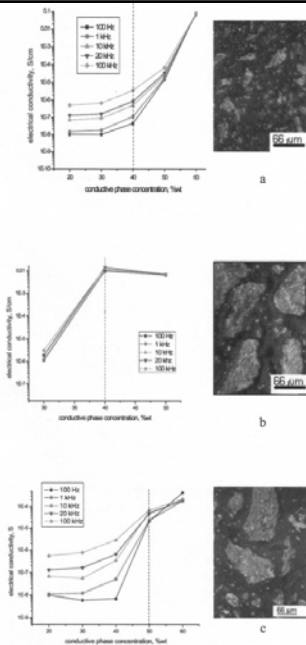


Fig. 2. Electrical conductivity and microstructural aspect of epoxy matrix composites function of the filler concentration and type: a)PP 900; b) PP/0.5SWNT 900; c) PP/1.5MWNT 900

4/21/2009

15

Ag nanowire ACF (Au seed, Co alignment)
 [Lin et al, ECTC'05]

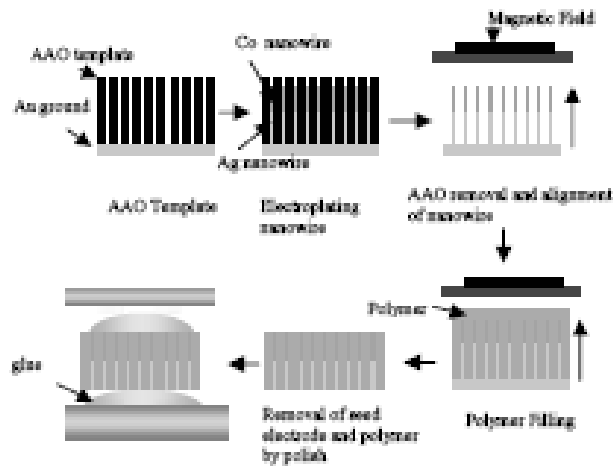


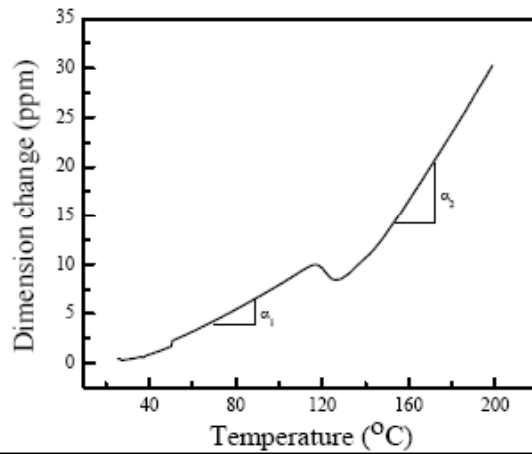
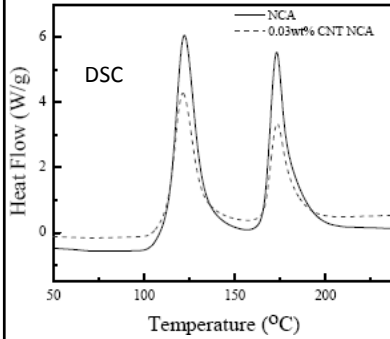
Fig. 1 Process Flow of Nanowire Conductive Film

4/21/2009

16

Addition of CNTs to NCAs: 0.03 wt% CNTs increases electrical and thermal conductivities c. 20%

NCA _s /NCF _s	CTE ppm/°C (α_1)	CTE ppm/°C (α_2)
No CNTs	71.55	197.2
0.02 wt% CNTs	62.3	179.8
0.03 wt% CNTs	60.9	177.8



Jiang, Min, Moon, & Wong, Proc. ECTC 2008 pp. 1385-1389

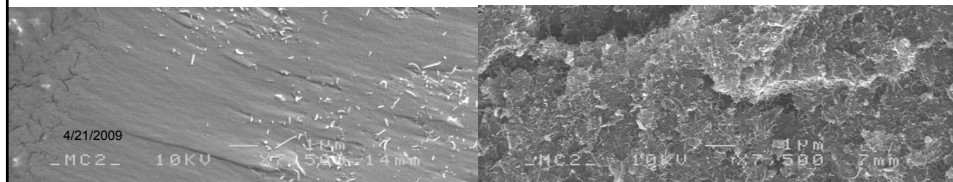
4/21/2009

Zhang, Jiang, Liu, & Inoue ICEPT/HDP 2008 E3-04 Effects of CNT & Ag powder addition

Sample	AF2 epoxy % matrix	3-10 μ m % Ag flakes	0.5-1 μ m % Ag powder	Vol % CNT	Resistivity $\mu\Omega$.cm
AgF201	60.762	38.238	1	0	45
AgF202	60.762	37.238	2	0	39
AgF203	60.762	36.238	3	0	40
AgF204	60.762	35.238	4	0	39
AgF205	60.762	34.238	5	0	48
AgF206	60.762	39.238	0	0	52
3F201	60.762	38.138	1	0.1	34
3F202	60.762	37.938	1	0.3	36
3F203	60.762	37.738	1	0.5	29

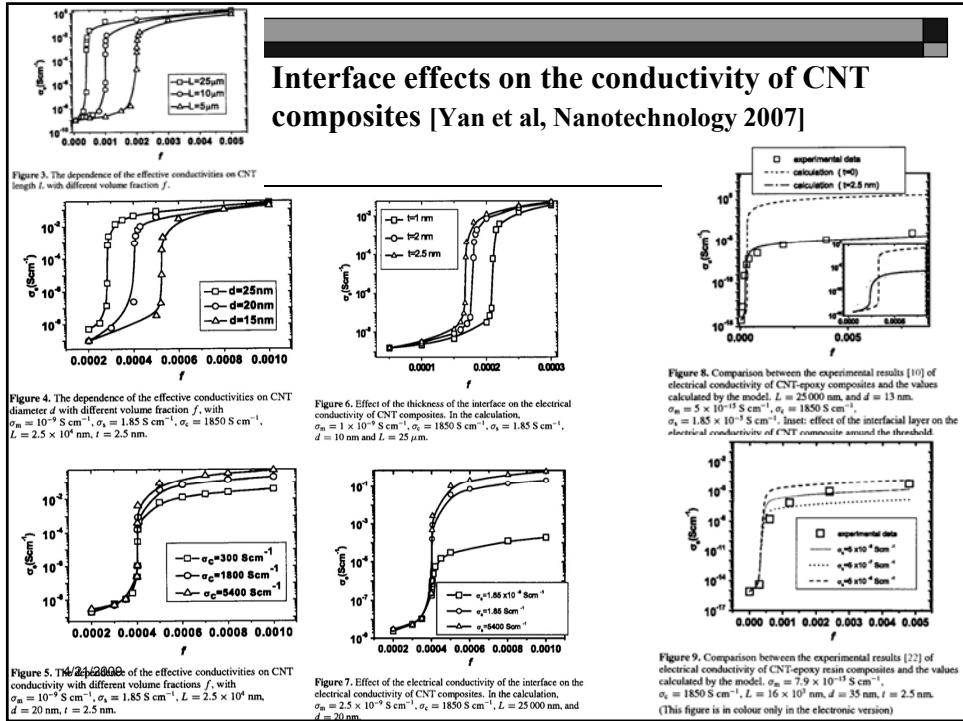
CNT dispersion in epoxy: (a) CNTs untreated

(b) CNTs treated H₂SO₄/HNO₃ 16hrs 50°C



4/21/2009

Interface effects on the conductivity of CNT composites [Yan et al, Nanotechnology 2007]



Microsprings (Ma et al)

Sputter deposition: Ti release layer

Sputter deposition: $\text{Mo}_{100}\text{Cr}_{20}$ (Stress-engineering)

Pattern interconnect by photolithography

Define release window

Etch release layer

Interconnect curls up automatically

2,568x 5.88 kV 10μm AMRAY #8882

30.0 kV 100μm SEM #881

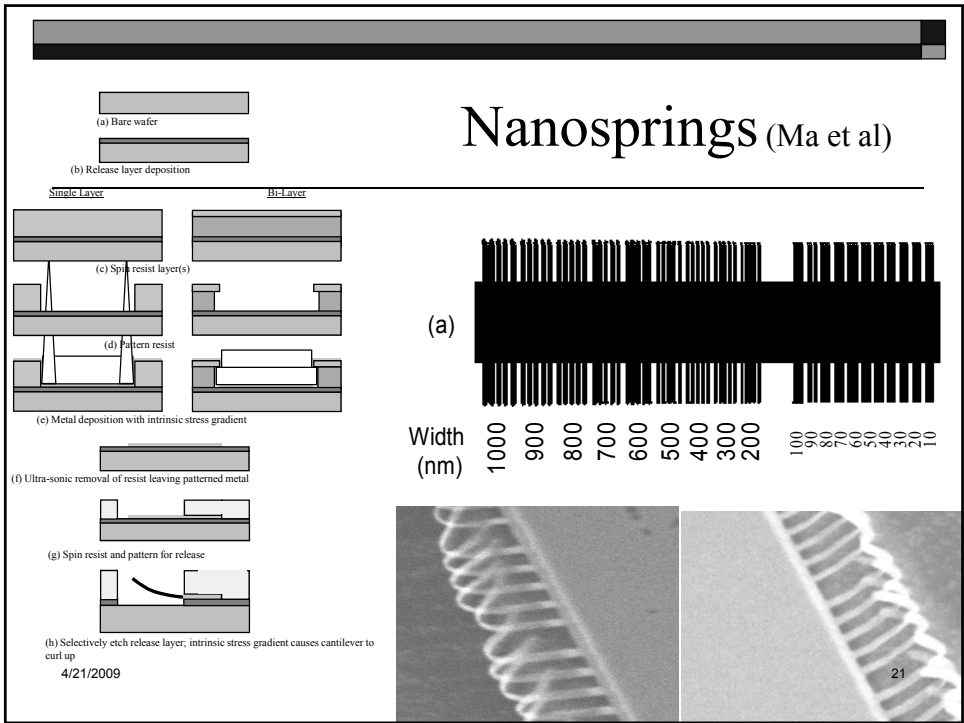
Ti Release layer

$\text{Mo}_{100}\text{Cr}_{20}$ metal

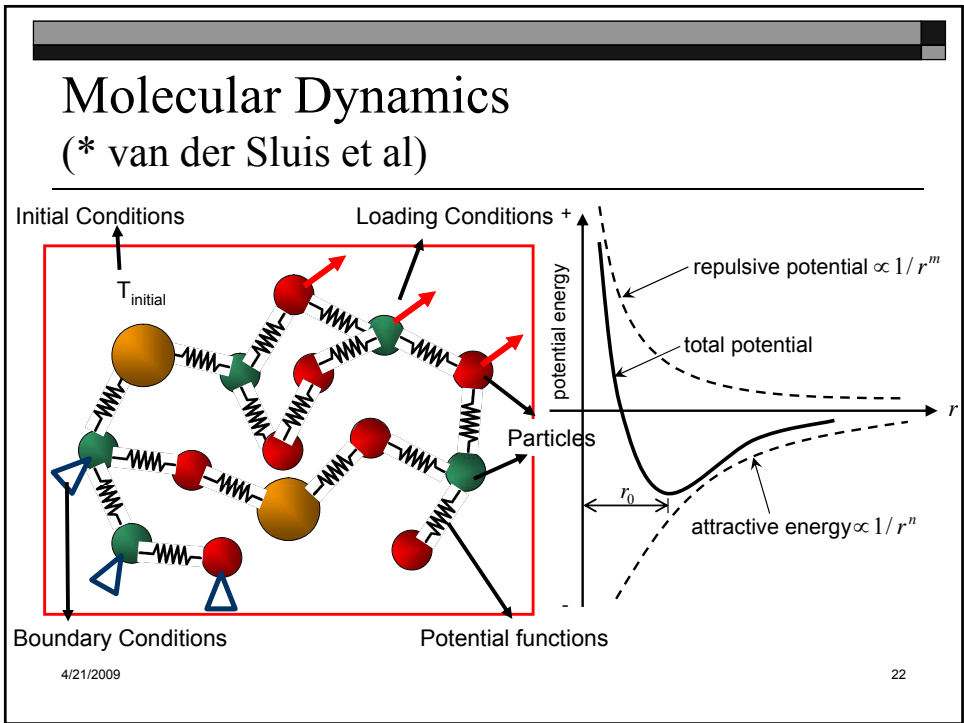
Substrate

Photoresist

Nanosprings (Ma et al)



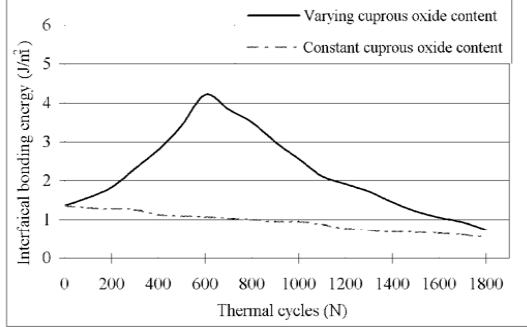
Molecular Dynamics (* van der Sluis et al)



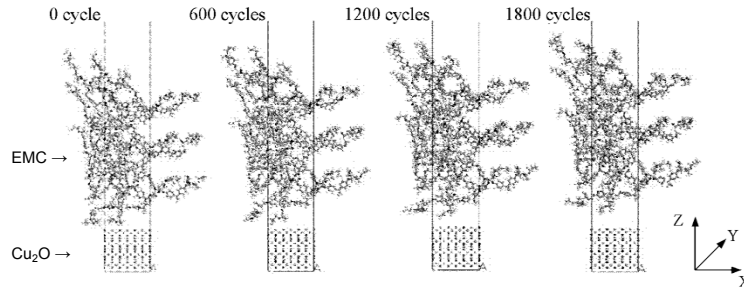
Molecular Dynamics

(* Fan & Yuen)

Modeling of interface H₂O diffusion, CNTs, etc



Adhesion increases with Cu₂O growth, decreases with void development



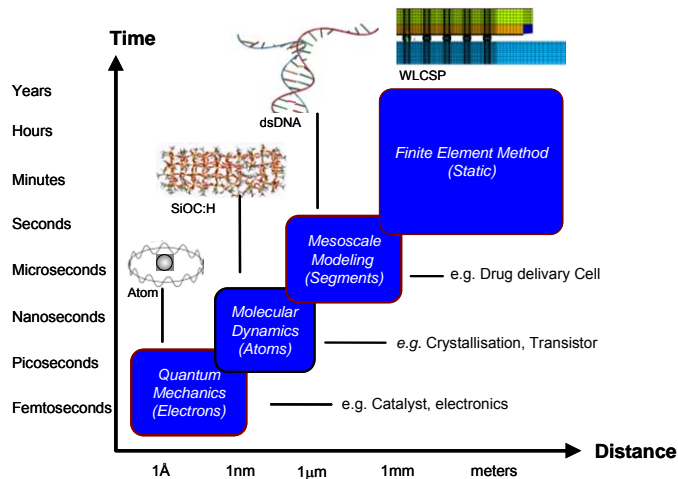
MD simulation snapshots of the Cu₂O/EMC system, showing void development at the interface

23

Nanoscale Modeling

(van der Sluis et al)

Molecular Dynamics; interscale interfaces



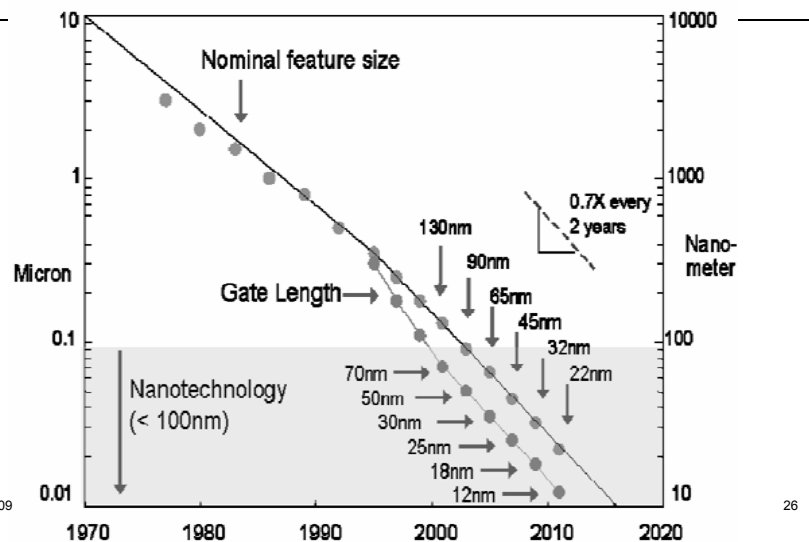
4/21/2009
Need software "interface" packages to transport modeling results between length scales

24

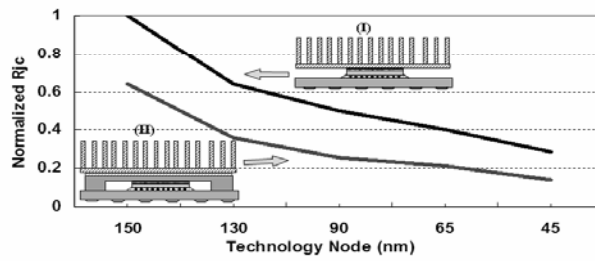
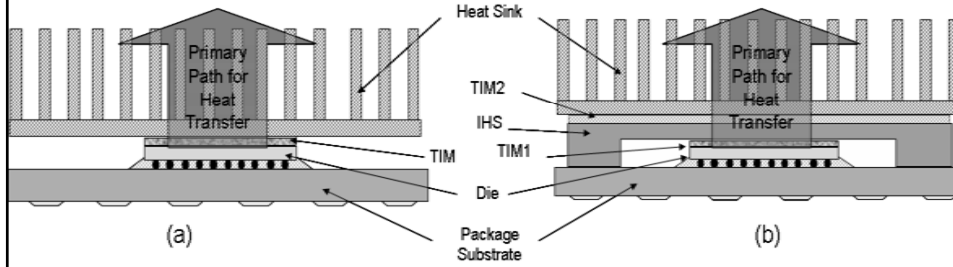
Nanoelectronics Packaging

- nm CMOS
- Single electron transistor (SET)
- Discussion: CNTs, molecular, RTDs, spintronics, etc
- Sensors

Nano-CMOS Packaging (Mallik)



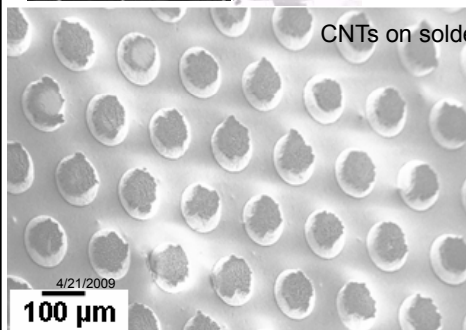
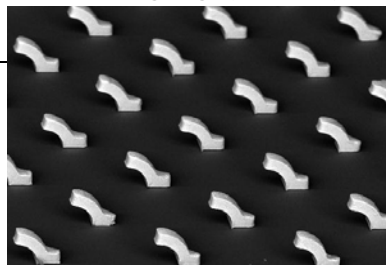
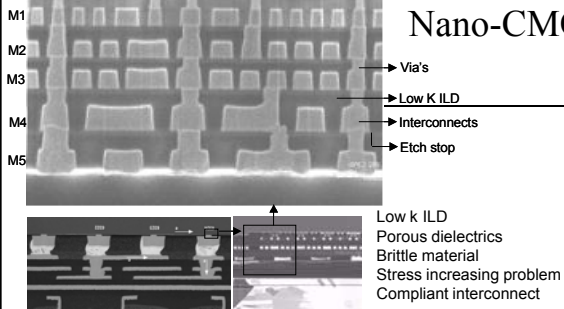
Nano-CMOS Packaging (Mallik)



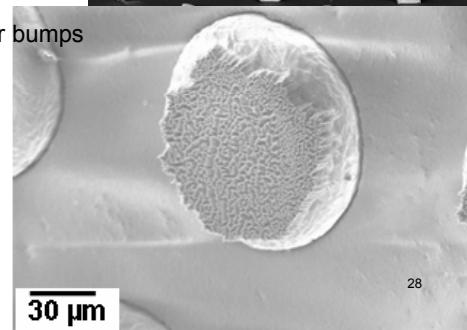
4/21/2009

27

Nano-CMOS Packaging (Mallik)

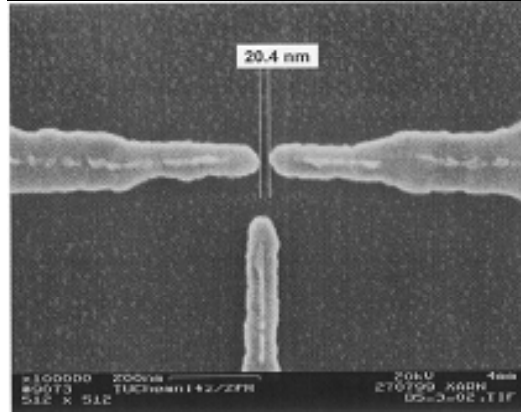


CNTs on solder bumps

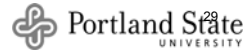
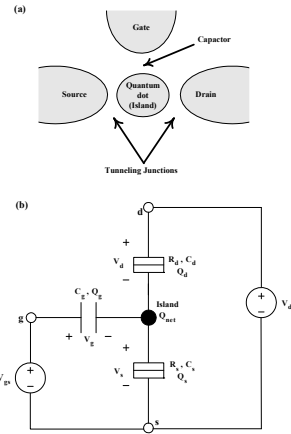


28

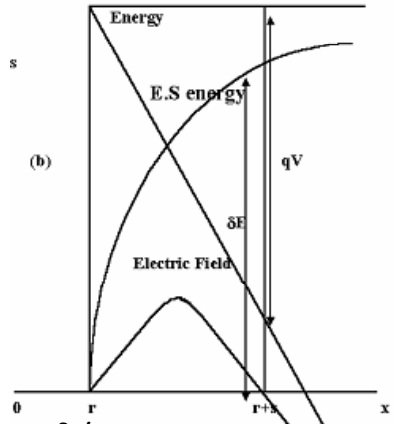
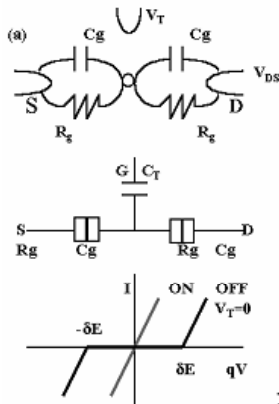
Single electron transistor (SET) as example Metal nanodot as simple SET example



Radehaus et al



Coulomb block & SET: Electric field & temperature



$T=0^{\circ}\text{K}$: abrupt threshold at $V=\delta E/q$

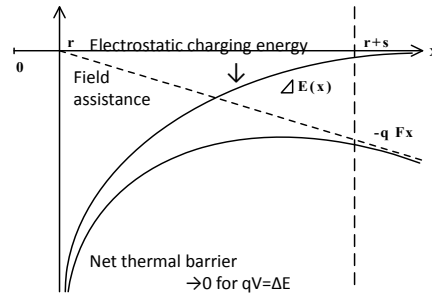
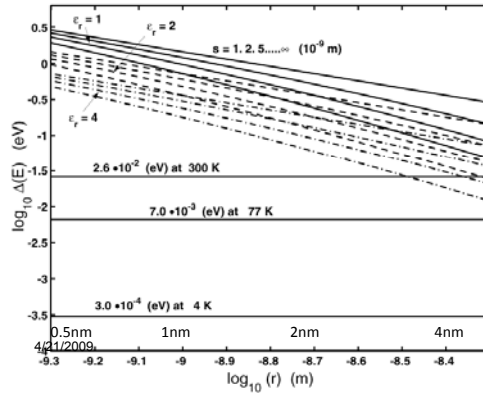
$T>0^{\circ}\text{K}$: randomly charged $\exp(-\delta E/kT)$

Nanoparticle Charging:

the Coulomb Block (Morris)

Spherical nanoparticles, radius r , separation s
Electrostatic charging energy:

$$\Delta E = \frac{q^2}{4\pi\epsilon} \rightarrow \frac{q^2}{4\pi\epsilon} \left[\frac{1}{r} - \frac{1}{r+s} \right]$$



31

Electrostatic activation/charging energy (usually stated $\delta E = q^2/4\pi\epsilon r$)

$$\delta E = (q^2 / 4\pi\epsilon)(r^{-1} - (r+s)^{-1}) - (2r+s)qF$$

$$\text{when } F < (q / 4\pi\epsilon)(r+s)^{-2}$$

and at high fields

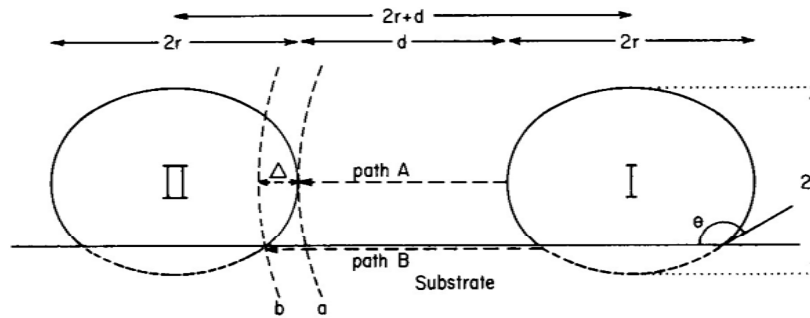
$$\delta E = (q^2 / 4\pi\epsilon)r^{-1} + (r/s)(2r+s)qF - (q^2 / 4\pi\epsilon s)^{1/2}((2r+s)qF)^{1/2}$$

$$\text{until } \delta E \rightarrow 0 \quad \text{when } qV = (1 + s/r)\delta E_{V=0}$$

4/21/2009

32

The geometry of 2 ellipsoidal nanodots of eccentricity $e = (1-(t/r)^2)^{1/2}$



33

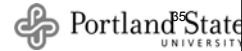
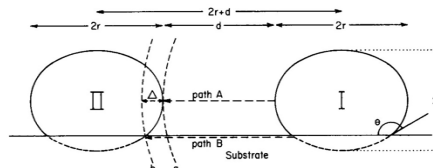
δE for oblate spheroids with applied field

- $\delta E = q^2/C$
 $= (q^2/4\pi\epsilon R)(2/e)[\sin^{-1}e - \sin^{-1}(e(1-p)/(1+p))]/(1-p) - qREa$
 for $E_a < E_{amin} = (q^2/4\pi\epsilon R)4p(1+p)^{-1}[(1+p)^2 - e^2(1-p)^2]^{-1/2}$, where $p = d/R$, $R = 2r+d$, and
- $\delta E = (q^2/4\pi\epsilon R)(2/e)[\sin^{-1}e - \sin^{-1}(e(1-p)R/((1-p)R+2x))]/(1-p) - qEax/p$
 for $E_{amin} < E_a < E_{amax} = (q^2/4\pi\epsilon R)4p(1-p) - 2(1-e^2)^{-1/2}$,
 where $x = \frac{1}{2}Re(1-p) \{ [(\{2qp/\pi\epsilon Ea(1-p)^2 R^2 e^2\}^2 + 1)^{1/2} + 1]^2 \}^{1/2} - e^{-1}$
- and $\delta E = 0$ at $E_a = E_{amax}$

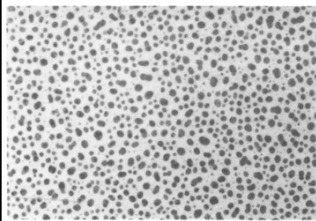


Mechanical stress effects

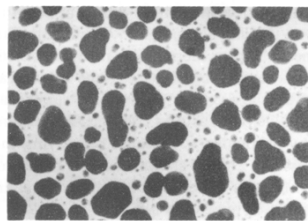
- Electron tunneling: $\sigma_0 = \text{const.} \times \exp(-4\pi d(2m^*\Phi)^{1/2})$
- Gauge factor $G=(2m\Phi)^{1/2}(4\pi d/h)$, if δE constant
- High gauge factor, approx. linear with d at low strain
- δE not constant
- Thermomechanical stress effects



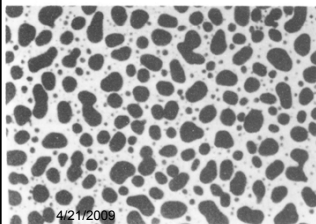
Discontinuous Metal Thin Films (DMTF)



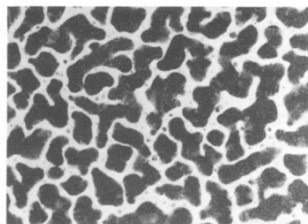
(a)



(c)



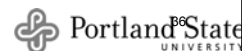
(b)



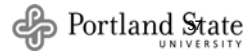
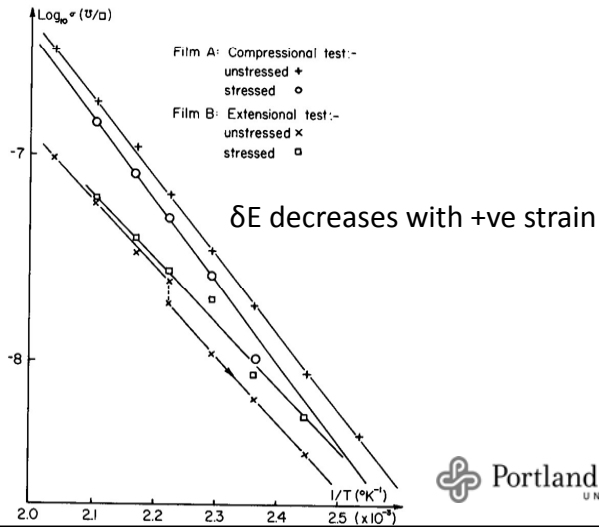
(d)

Kazmerski & Racine, 1975

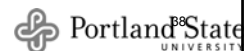
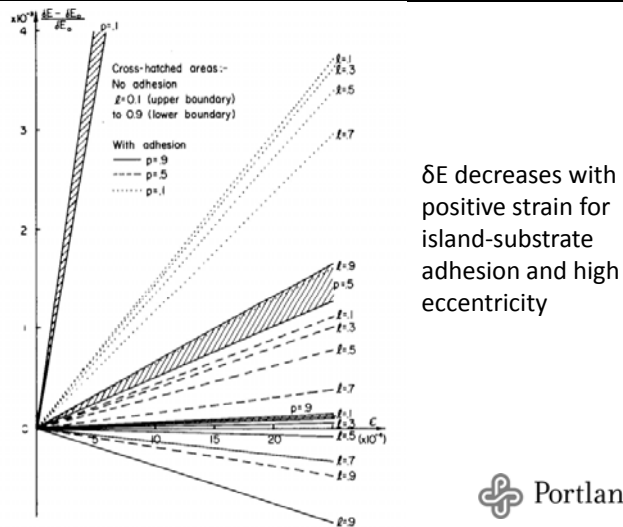
- Formation (e.g. Au/glass)
- nm islands
nm gaps
- Well researched 1960's-1970's
- Electron tunneling
Charging energy
- Coulomb blockade
nanodots in series
- $\sigma = \sigma_0 \exp(-\delta E/kT)$



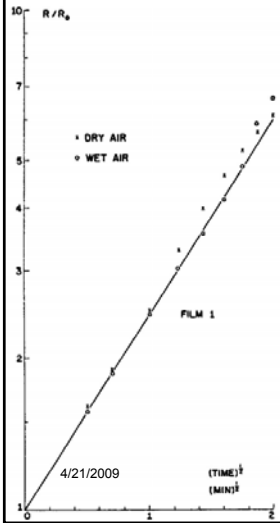
DMTF strain effects: experimental



DMTF strain effects: theoretical δE variation

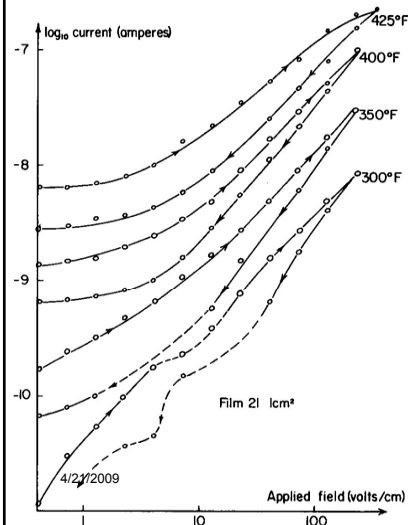


DMTF resistance variation upon exposure to air (oxygen)



- Other gases
- Surface adsorption increases metal work function
- Tunneling barrier height increases
- Substrate diffusion
- Environmental stability
- Encapsulation

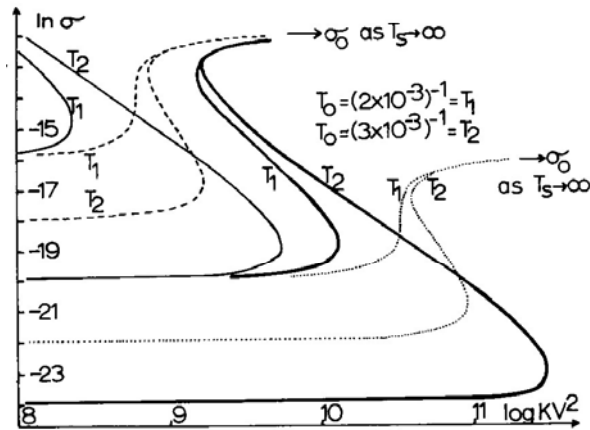
DMTF current variation with voltage cycling



- Electrical stability
- Ion drift or substrate polarization
- Surface conduction

Thermal Stability: DMTF switching

- NDR inherent in all negative TCR materials
- Thermal runaway
- Other switching mechanisms
- N-type & S-type

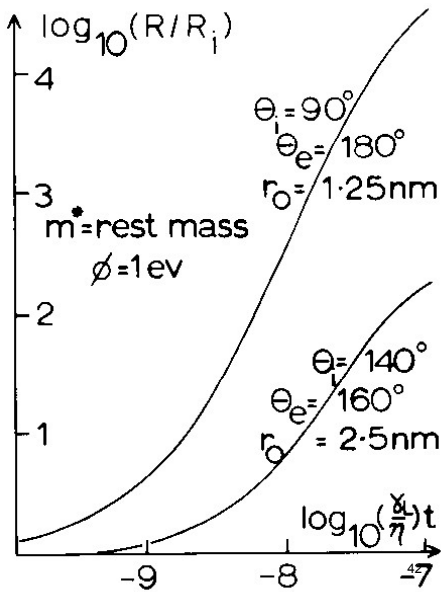


4/21/2009

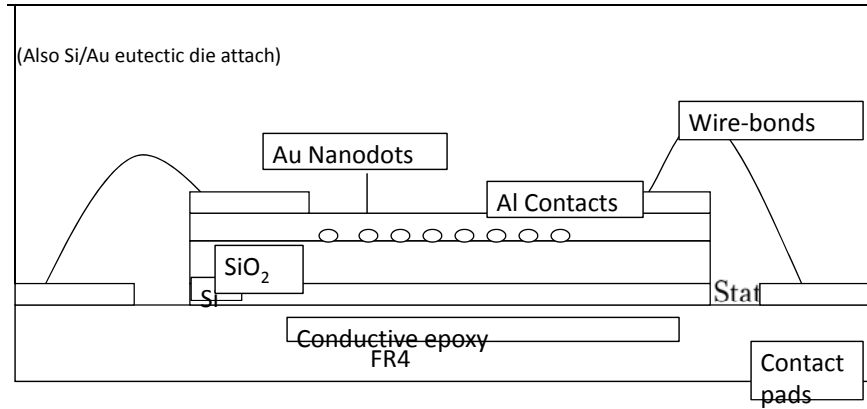
41

Structural Stability

- Coalescence
- DMTF R(t) model
 - adatom collection
 - surface self-diffusion



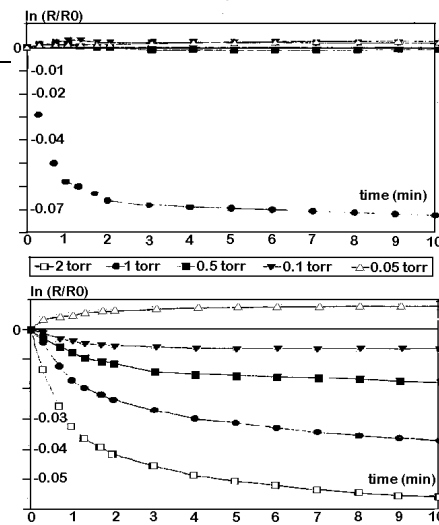
Schematic of reliability test sample



43

Embedded Package Reliability Sensors

- DMTF strain sensor
 - See back
- H₂ Sensor for corrosion
- Discontinuous Pd film
 - Work function increases → resistance increases
 - Islands swell → gaps narrow → resistance decreases



4/21/2009

44

Summary

- Nanopackaging materials (electrical, mechanical, thermal):
 - Nanoparticle applications
 - Carbon nanotube (CNT) applications
 - ECAs
 - Nanowires, nanospring contacts
 - Modeling: Molecular Dynamics to Effective Medium
- Nanoelectronics
- Health & environment: CNTs in the body, nano-Ag toxicity to bacteria
- “Nanopackaging: Nanotechnologies in Electronics Packaging,”
J.E. Morris (editor) Springer (August 2008)

